

*Full Length Research Paper*

## **Successive off take of elements by maize grown in pure basalt powder**

**Luise Lottici Krahl<sup>1\*</sup>, Simone Patrícia Aranha da Paz<sup>2</sup>, Rômulo Simões Angélica<sup>2</sup>, Leonardo Fonseca Valadares<sup>3</sup>, José Carlos Sousa-Silva<sup>4</sup>, Giuliano Marchi<sup>4</sup> and Éder de Souza Martins<sup>4</sup>**

<sup>1</sup>Department of Environmental Science, Universidade de Brasília, Área Universitária, 01, Vila Nossa Senhora de Fátima, CEP: 73345-010 - Planaltina - DF, Brazil.

<sup>2</sup>Instituto de Geociências, Universidade Federal do Pará, Caixa Postal 1611, CEP: 66075-110, Belém - PA, Brazil.

<sup>3</sup>Embrapa Agroenergia, Parque Estação Biológica - PqEB s/nº. Caixa Postal 40.315, CEP: 70770-901 - Brasília - DF, Brazil.

<sup>4</sup>Embrapa Cerrados, Rodovia BR-020, Km 18, Caixa Postal 08223, CEP: 73310-970 – Planaltina - DF, Brazil.

Received 21 October, 2019; Accepted 11 December, 2019

**Basalt powder wastes from mining activities have potential to be used as a natural fertilizer. Basalt minerals in agricultural soils may release plant nutrients and increase soil negative charge. In this work, the weathering of basalt promoted by maize rhizosphere was investigated. We studied the chemical and mineralogical composition of basalt, including cation exchange capacity, as well as the rate of elements offtake by maize grown in a pure basalt powder during seven successive growth cycles. A pot experiment was carried out under controlled environmental conditions; plant and rock materials were evaluated at the end of successive growth cycles. X-ray powder diffraction analysis showed diopside and andesine as main minerals of basalt, and smectite. Scanning electron microscopy images evidenced new amorphous components resulting from rhizosphere-induced weathering. The elements K, Ca, Mg, Al, B, Cu, Fe, Mn and Zn were measured in plant tissue, and related to the weathering of basalt minerals. The studied basalt, therefore, provides nutrients to plants and exhibits physicochemical properties, such as cation exchange capacity, especially important for highly weathered soils presenting low cation exchange capacity, such as Oxisols.**

**Key words:** Bioweathering, natural fertilizer, mining waste, basalt minerals, cation exchange, nutrient availability.

### **INTRODUCTION**

Some silicate minerals contain high concentration of nutrients, which are required by plants for growth. These minerals have been used as agricultural fertilizers, releasing its nutrients slowly (Ciceri and Allanore, 2019;

Manning et al., 2017; Zorb et al., 2014). In the recent years, many studies where mining by-products were applied to soils have emerged, turning mining waste in products as a soil fertilizer or remineralizer. The approach

\*Corresponding author. E-mail: [luisekrahl@yahoo.com.br](mailto:luisekrahl@yahoo.com.br)

is an attempt to reduce agricultural costs and dependence on imported fertilizers. Many works showed positive results for crop productivity and increases in soil quality, whereby basalt powder, for its composition and abundance in spread areas over the world, may assist massively in quality building of soils (Anda et al., 2015; Nunes et al., 2014; Silva et al., 2017). In Brazil, an existing network of basalt quarries, already producing construction aggregates at low cost, has the potential to supply crushed material to agricultural regions (Lefebvre et al., 2019).

Basalts are among the most studied rocks because it provides nutrients for plants, especially calcium (Ca), magnesium (Mg), potassium (K) and micronutrients, such as boron (B), copper (Cu), manganese (Mn) and zinc (Zn) (Anda et al., 2015; Chaturika et al., 2015; Ramos et al., 2015). Plants rhizosphere and their associated microbial populations play a major role in the silicate minerals weathering (bioweathering) by increasing acidity, absorbing and releasing elements and organic ligands, as well as siderophores (Burgehelea et al., 2015). Plant roots, ultimately, contribute to increase the dissolution rates of Ca and Mg silicates present in basaltic minerals (Akter and Akagi, 2005; Anda et al., 2015; Hinsinger et al., 2001; Silva et al., 2017).

Basalt minerals undergo a congruent dissolution whenever its bulk chemical composition is rich in iron (Fe), and alkaline earth elements, such as Mg and Ca (Silva et al., 2017). The susceptibility of basalt minerals to weathering, generally follows the sequence: glass > olivine > pyroxene > amphibole > plagioclase > K-feldspar (Eggleton et al., 1987). The Fe(II) oxidation is a driving force in primary mineral weathering (Essington, 2003). As an intermediate step, at an early stage of weathering of basic silicate minerals, the rapid oxidation of Fe(II) can form amorphous phases and low crystallinity minerals, such as ferrihydrite (Colombo et al., 2014; Yu et al., 2017), which is formed from solution precipitates. In time, the weathering of these minerals may become a mixture of ferrihydrite, iron oxide-hydroxides and clay minerals. Some phases may be slowly recrystallized forming secondary minerals. During weathering, some of the basalt minerals may be converted into smectites. Ferromagnesian minerals form trioctahedral smectite, whereas plagioclase alters to dioctahedral smectite.

In weathered basalts, pyroxenes also weather via a mechanism involving a high degree of structural inheritance. The mechanism can be induced by grinding particles to an ultra-fine size (Berner and Schott, 1982). When the surface of these particles, in diopside, suffers cation depletion followed by deprotonation, an incongruent dissolution takes place, and secondary minerals, normally smectite, are formed (Berner and Schott, 1982).

The application of a finely ground basalt in a highly weathered soil increases its cation exchange capacity. Anda et al. (2015) verified, after a high dose (80 t basalt

ha<sup>-1</sup>) was applied in a Malaysian Oxisol, a sharp increase in the soil's net negative charge was observed from 1.5 to 6.3 cmol<sub>c</sub> kg<sup>-1</sup> in a 12-month incubation period, and to 10.1 cmol<sub>c</sub> kg<sup>-1</sup>, after 24 months. The increasing net negative charge rate suggest that smectite like minerals or low crystallinity minerals, which is a source of permanent negative charge, were formed. An increase in permanent negative charge in Oxisols is an invaluable gain for its quality. However, basalt composition is very dissimilar among different source locations and its charge contribution to soils, as well as rate of transformation or dissolution will depend on the basalt composition and texture, and on abiotic and biotic conditions.

Most natural tropical soils - such as Brazilian Oxisols - due to the strong weathering and intense leaching processes become acidic, with low fertility and low cation exchange capacity. Thus, the management of these soils with crushed rocks should be focused on increased surface charge characteristics and cation retention. We hypothesize that crushed basalt applied to agrosystems release beneficial elements for crop growth and generate new negative charge sites in the soil. Hence, the knowledge of physicochemical properties of basalt powder and how the rhizosphere of cultivated plants affects the weathering of basalt minerals is a requirement to understand its potential benefits to agricultural soils. The aim of this work was to investigate changes in the chemical and mineralogical composition of basalt powder, including cation exchange capacity, as affected by the rhizosphere of maize, as well as the rate of elements offtake.

## MATERIALS AND METHODS

### Sampling

A basalt sample was collected from piles located at Araguari, Minas Gerais State, Brazil (Moraes et al., 2018). This is a by-product that originated from the production of gravel for civil construction. The sample was air dried and was homogenized using the cone-and-quartering reduction method (Campos and Campos, 2017). This procedure was repeated several times to ensure complete homogenization of material, forming the bulk sample.

### Greenhouse experiment

The pure bulk basalt sample was placed into 500 mL pots under controlled environmental conditions in a greenhouse. Two plants of maize (*Zea mays*) per pot were grown in sets of three pots, repeated for seven growth cycles, totaling 21 pots. Each growth cycle was 45 days. Seven extra pots without plants were prepared, as a control treatment. At every two days, all pots were watered with deionized water. Pots were fertilized with nutrient solution (92.76 mg pot<sup>-1</sup> NH<sub>4</sub>H<sub>2</sub>PO<sub>4</sub>) in the 15<sup>th</sup> and 30<sup>th</sup> days of growth of each cycle.

At the end of each 45-days cycle, whole plants from all pots were harvested. The basalt content from one set of three pots previously grown with plants, and another, from one pot of the control set were removed from the greenhouse. The pots content was used for the laboratory analyses. The remaining sets were re-sown for a new growth cycle.

## Plant analysis

The harvested plants were oven dried at 65°C until constant weight. The dry biomass was taken. Major (K, Ca, Mg, Al, Fe) and minor elements (B, Cu, Mn e Zn) in dry biomass (total dry mass comprising shoots and roots) were extracted by HNO<sub>3</sub>:HClO<sub>4</sub> in a digestion block, according to Embrapa (2017) and determined by inductively coupled plasma-optical emission spectrometry (ICP-OES).

Elements offtake (plant element concentration x dry mass) along the cycles were modelled and the equations were selected according to the analysis of variance (ANOVA) and, thereafter, were tested for normality (Shapiro-Wilk) and constant variance test (homoscedasticity). These statistical analysis were performed using Sigma Plot 12.0 software (Sigma Plot Software; San Jose, California, USA).

Dry mass and elements offtake were analyzed by Principal Component Analysis (PCA), using standardized scores. The RStudio software (version 3.4.0) was used along with its PCA packages FactoMineR and factoextra.

## Rock material analysis

The basalt pots removed from the glasshouse at the end of each growth cycle were dismantled and its contents were wet sieved to obtain four size fractions: < 53 µm, 53-300 µm, 300-1000 µm and > 1000 µm.

The main chemical elements of basalt were analyzed using the multi-acid solution method, where: 500 mg of sample was digested in 2:3:2:1 ratio of HCl:HNO<sub>3</sub>:HF:HClO<sub>4</sub>; 10:15:10:5 mL, respectively, determined by ICP-OES (SGS Geosol Laboratórios Ltda). Major elements were determined by wavelength dispersive X-Ray Fluorescence (XRF) spectroscopy, on fused glass discs, 40 mm-diameter, prepared from 0.8 g of sample powder mixed with 4.5 g lithium tetraborate flux and fused in Pt-5% Au crucibles at 1120°C (SGS Geosol Laboratórios Ltda). The loss on ignition was determined after heating samples overnight at 105°C to remove water. The weight loss was measured after calcination of samples at 1,000°C for approximately 2 h.

The mineralogical composition of fractions < 53 µm was analyzed by X-ray diffraction analysis (XRD) using a PANalytical Empyrean (PW3050/60) diffractometer, using the powder method in the range of 5° < 2θ < 75°. CoKα radiation (40 kV; 40 mA) was applied, and the 2θ scanning speed was set at 0.02° s<sup>-1</sup>. Data was acquired using the software X'Pert Data Collector 4.0 and the data were treated on X'Pert HighScore 3.0 (PANalytical). Minerals were identified by comparing the obtained diffractogram with the ICDD-PDF (International Center for Diffraction Data) database.

The X-ray diffraction pattern of the clay fraction (oriented sample) was obtained three times: the first was air-dried, the second was after treatment with ethylene glycol, and the third was after heating at 550°C for 2 h.

The mineralogical composition in each basalt size fraction was estimated by the stoichiometric method, also known as rational calculation, which is based on the relationship of the experimental chemical composition with the chemical formulas of the minerals, establishing logical considerations based on the qualitative (XRD) and quantitative (XRF) analytical data. An already well-known software used to perform the rational calculation is the ModAn (Paktunk, 1998), which was used in this work.

The morphology of the basalt bulk samples was examined by scanning electron microscopy (SEM) using a Zeiss field emission microscope model SIGMA HV using the InLens detector. A thin conductive layer of gold (10 nm) was deposited over the samples using the Q150T-ES sputter (Quorum Technologies). The chemical composition of selected mineral particles was evaluated by Energy-dispersive X-ray spectroscopy (EDS).

Cation exchange capacity on the fractions < 53 µm was determined by magnesium sorption (BS EN ISO 11260, 2011). Measurements of the CEC followed the methodology: 3.5 g of sample were placed in 50 mL polyethylene tubes, and leached with 30 mL 0.1 mol L<sup>-1</sup> barium chloride dihydrate for 1 h. Tubes were centrifuged and the supernatant was removed. The procedure was repeated three times. Samples were, then, equilibrated with 30 mL 0.01 mol L<sup>-1</sup> barium chloride solution, and shaken for 12 h. Tubes were centrifuged and the supernatants were removed. Subsequently, 30 mL 0.02 mol L<sup>-1</sup> magnesium sulfate heptahydrate was added and shaken for 12 h. Tubes were centrifuged and supernatant was collected for analysis. The excess magnesium was determined by flame atomic absorption spectrometry (FAAS AA-6300 Shimadzu). Triplicates were used.

## RESULTS AND DISCUSSION

The X-ray fluorescence (XRF) analysis showed that the chemical composition in basalt fractions (Table 1) was nearly uniform (Tables 2 and 3). The amount of SiO<sub>2</sub> and Al<sub>2</sub>O<sub>3</sub> reflects the presence of minerals such as andesine [(Ca,Na)(Al,Si)<sub>4</sub>O<sub>8</sub>], a plagioclase feldspar, and diopside [MgCaSi<sub>2</sub>O<sub>6</sub>], a monoclinic pyroxene. A high content of Fe<sub>2</sub>O<sub>3</sub> comes from diopside and ilmenite [FeTiO<sub>3</sub>]. Significant concentration of CaO and MgO was found in all grain sizes, when compared to the basalt composition applied as fertilizers in another studies (Nunes et al., 2014; Ramos et al., 2015), even though basalt chemical composition varies widely.

Basalt mineralogy is dominated by andesine and diopside (Figure 1). After 315 days in presence or absence of plants, basalt mineralogy remained unchanged. The reflections of andesine and diopside minerals showed little changes in the X-ray patterns and there were detected no secondary crystalline minerals after seven maize growth cycles.

The XRD analysis of the clay fraction as analyzed on oriented mount (Figure 2) revealed the typical shift of the *d*<sub>001</sub> peak from 15.9 Å (in the air-dried state) to 17.7 Å (in the ethylene glycol state), indicating the presence of smectite, which was found in different proportions among the basalt fractions (Table 3). After heating, the typical collapse to 9.9 Å is observed.

An important parameter in the dissolution rate and nutrient release of primary minerals is the grain size and its relationship with the exposed reactive surface of minerals and with the chemical composition. The smallest grain sizes are the most reactive fractions (Basak, 2018; Bray et al., 2015).

The crystalline phases on < 53 µm size fraction of the mineral were composed of 48.2% of andesine that has also calcium in its structure (Table 3 and Figure 3). However, andesine has high structural stability and is not easily weathered as it presents a great proportion (Al/Si = 0.5 – 0.66) of Al in its structure. It would be expected that the dissolution of andesine was incongruent, releasing alkalies and alkaline earths relative to silica and alumina.

Diopside represents 20.5% of <53 µm sample. Depending on milling size, and environmental conditions,

**Table 1.** Particle size distribution of the basalt powder used in the experiment.

Sample	Particle size distribution ( $\mu\text{m}$ )				Total (g pot <sup>-1</sup> )
	< 53	53 - 300	300 - 1000	> 1000	
	-----%-----				
Basalt powder	10.67	12.44	26.5	50.39	663.69

**Table 2.** Chemical composition of the basalt powder (fractions and bulk) determined by XRF and ICP-OES.<sup>1</sup>

Fraction ( $\mu\text{m}$ )	SiO <sub>2</sub>	Al <sub>2</sub> O <sub>3</sub>	Fe <sub>2</sub> O <sub>3</sub>	CaO	MgO	TiO <sub>2</sub>	P <sub>2</sub> O <sub>5</sub>	Na <sub>2</sub> O	K <sub>2</sub> O	MnO	BaO	Cr <sub>2</sub> O <sub>3</sub>	Cu	Mo	Zn	LOI <sup>2</sup>
	-----%-----												----- mg kg <sup>-1</sup> -----			
< 53	49.4	12	16.5	7.38	6.35	2.74	0.35	1.72	0.97	0.16	0.06	<0,01	206	<3	116	2.57
53 - 300	49	11.3	16.2	7.91	5.91	2.84	0.36	1.73	0.95	0.19	0.06	0.01	196	<3	131	1.55
300 - 1000	49.4	12.2	15.5	8.53	5.4	3.24	0.4	1.95	0.98	0.19	0.06	0.01	194	<3	134	0.93
> 1000	49.4	12.7	15.1	8.85	4.9	3.38	0.4	2.46	0.93	0.2	0.05	0.01	211	<3	149	0.58
Content bulk <sup>3</sup>	49	12.6	15.4	8.73	5.28	3.2	0.43	2.06	0.9	0.2	0.06	<0,01	208	<3	139	1.32

<sup>1</sup>SGS Geosol Laboratórios Ltda; <sup>2</sup>Loss on ignition; <sup>3</sup>Original sample.

**Table 3.** Mineralogical composition of the basalt powder (fractions and bulk).

Fraction ( $\mu\text{m}$ )	Andesine (%)	Diopside (%)	Ilmenite (%)	Smectite (%)
< 53	48.2	20.5	18.0	13.2
53 - 300	47.0	24.5	18.3	10.2
300 - 1000	50.7	24.9	18.0	6.3
> 1000	53.1	25.7	17.9	3.3
Content bulk <sup>1</sup>	51.9	25.7	18.1	4.3

<sup>1</sup>Original sample.

the diopside is relatively, an easily weatherable mineral, and after being applied to agricultural soils, may become a source of Ca and Mg for crops in diopside rich basalts (Figure 3). Moreover, diopside is unstable under acidic conditions and may dissolve congruently by weathering in such conditions (Wilson, 2004). The rhizosphere is the environment where diopside dissolution is likely to occur. The dissolution of pyroxenes is controlled by reactions at the mineral surface. By structural reasons, Ca, Mg and Fe are released preferentially at the beginning, and, lately, the dissolution becomes congruent and linear, as the weathering proceeds. The dissolution products could be precipitated as amorphous compounds, not detectable by XRD (Berner and Schott, 1982).

Diopside and ilmenite (18% of <53  $\mu\text{m}$  fraction) comprise the major iron-containing minerals in the basalt sample (Figures 1 and 3). Iron rich minerals are also rich in micronutrients such as Mn, B, Cu, and Zn.

A representative amount of a smectite (13.2%), mainly in the <53  $\mu\text{m}$  fraction was present in the basalt. Smectite is an expansive clay that has a high cationic exchange

capacity (CEC). As particle size increases, the presence of smectite decreases (Table 3). Probably, the weakest cleavage faces on basalt particles are those richer in smectite. Non-weathered samples from basalt presented 24.85 ( $\pm 1.16$ )  $\text{cmol}_c \text{kg}^{-1}$  on < 53  $\mu\text{m}$  size fraction. The smectite is a secondary mineral of the phyllosilicate class responsible for most of the reactivity of the studied basalt. As a matter of comparison, the CEC values of the montmorillonites range between 70 and 120  $\text{cmol}_c \text{kg}^{-1}$ , while the CEC values for the vermiculites range between 130 and 210  $\text{cmol}_c \text{kg}^{-1}$  (Essington, 2003). Also, Oxisols from Cerrado present CEC  $\sim 9.4 \text{ cmol}_c \text{kg}^{-1}$  (STD = 3.9), and some are as low as 4.1  $\text{cmol}_c \text{kg}^{-1}$  at pH 7.0 (Marchi et al., 2015). These soils present variable charge and natural pH is lower than 5, with effective CEC to even lower values. Therefore, inputs materials containing elevated surface area and permanent negative charge in these soils may represent a great gain in quality.

Total plant biomass production decreased along each successive cycle (Equation 1), with highest production in the first crop cycle (4.15 g of dry matter) and the lowest in

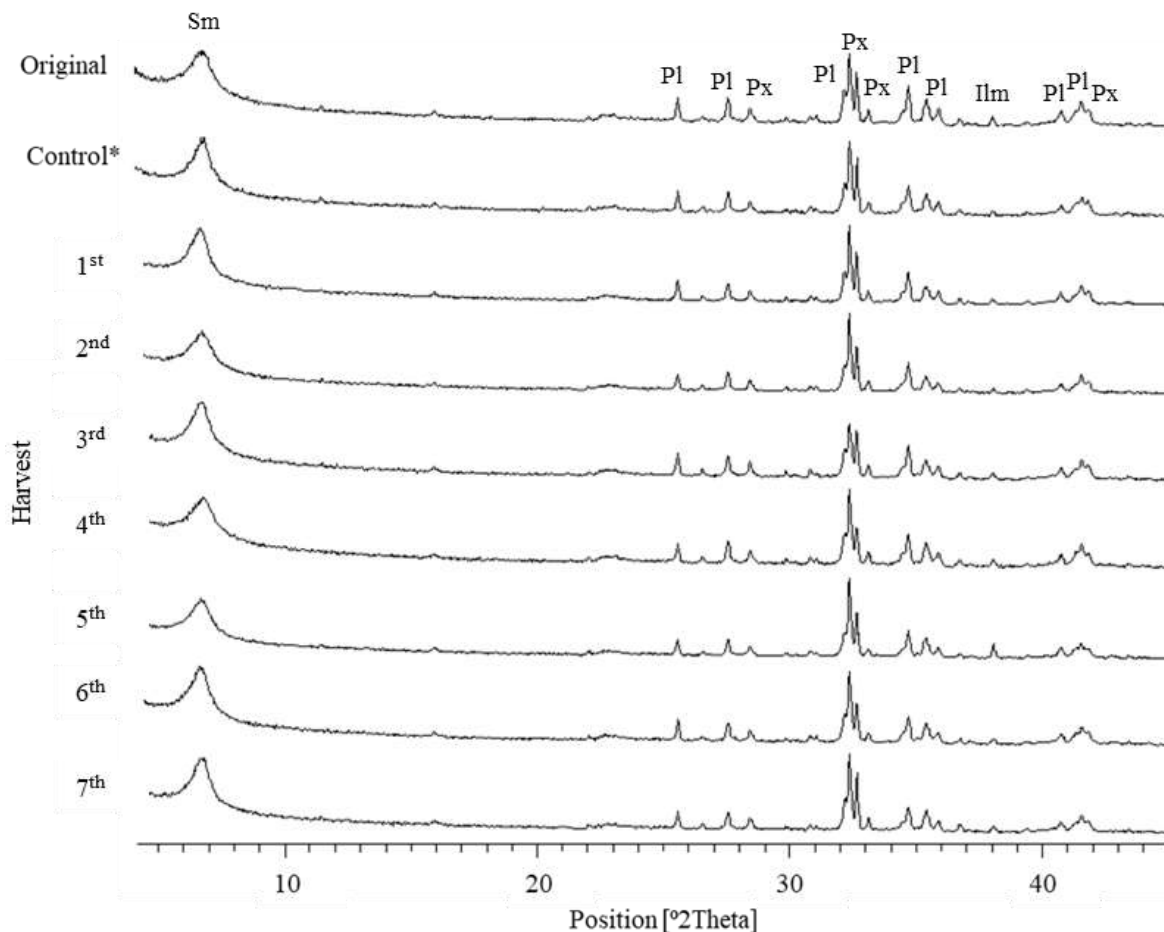


**Figure 1.** X-ray diffraction patterns of <53  $\mu\text{m}$  size particles of basalt after interaction with maize rhizosphere evidencing andesine (Pl), diopside (Px), smectite (Sm) and ilmenite (Ilm) minerals during 7 harvest crops; Control is the basalt collected from the pot without plants at the end of the experiment.

the last cycle (1.22 g of dry matter; Figure 4). Although plants were grown in pure rock, they were able to grow and take up some macro and micronutrients from basalt in its natural pH (9.04 - 6.99).

$$\text{Dry mass (g per pot)} = 4.54^{**} - 0.44^{**}(\text{cycle}), R^2 = 0.96 \quad (1)$$

The amount of nutrients taken up from basalt by plants varied over each crop cycle (Figure 4). These differences in element mobilization were related to dissolution kinetics of specific minerals. Potassium uptake showed a diverse dynamic than the other elements (Figure 5). Probably, K was extracted by plant roots from non-exchangeable sites from interlayers of smectite minerals, other than by dissolution, such as Ca and Mg. Slowly available potassium, which is fixed and non-exchangeable, is trapped between the layers or sheets of K-rich 2:1 minerals. The idea was clarified statistically by the principal component analysis (PCA) where K, with similar statistical contribution than the other elements to describe results, pulls up toward the y-axis, pulling dry

matter in between (Figure 6). The PCA indicated that K presents a different mechanism of release from rock and it reflects on the interaction among the other nutrients.

After applied to soils, the layers from 2:1 minerals may adsorb and release cations, but their efficacy will also depend on the mineral particle size. Indeed, several studies show the presence of 2:1 clay size minerals, even in subsidiary quantities, increases effectively the retention of cations in soil (Raheb and Heidari, 2011).

Plants have developed several highly specific mechanisms to acquire K from minerals (Samal et al., 2010). Wang et al. (2000) investigated the ability of plant types to extract and uptake K from slightly weathered gneiss of differing particle sizes. The authors showed that, among the studied plant species, maize was the one that extracted the highest amount of K.

Concentrations of K in maize dry mass varied from 2.6 to 15 g K kg<sup>-1</sup> of dry weight. The results demonstrate that the plants were able to access some K from basalt to sustain growth. The K requirement for optimal maize growth range is 17.5 to 22.5 g kg<sup>-1</sup> in vegetative parts

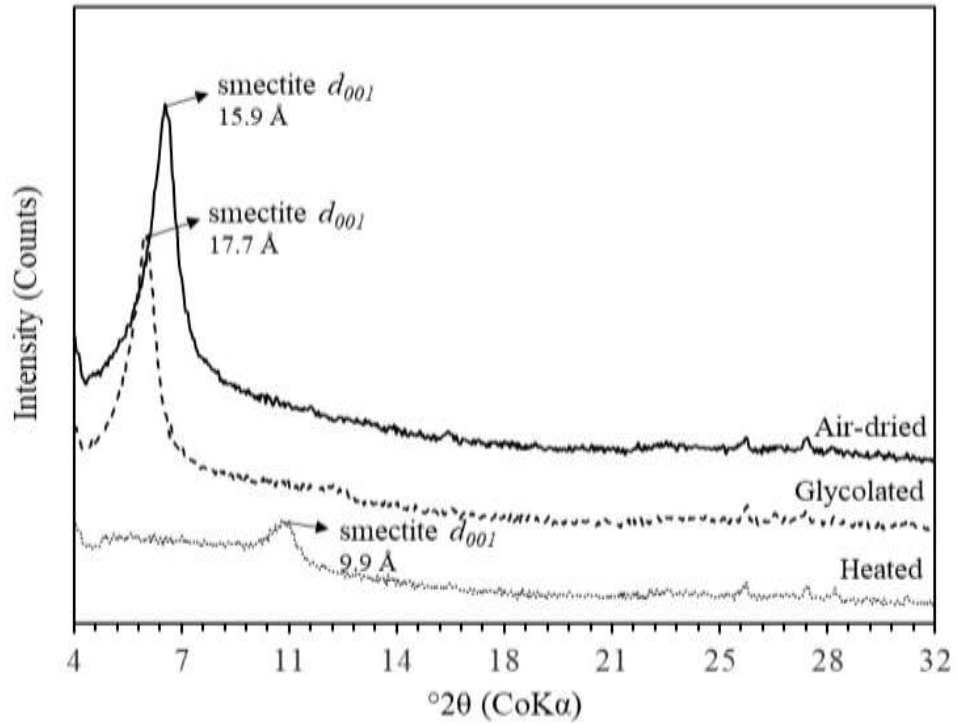


**Figure 2.** X-ray diffraction patterns of the clay fraction (oriented sample) obtained three times: air-dried, after treatment with ethylene glycol, and heated at 550°C.

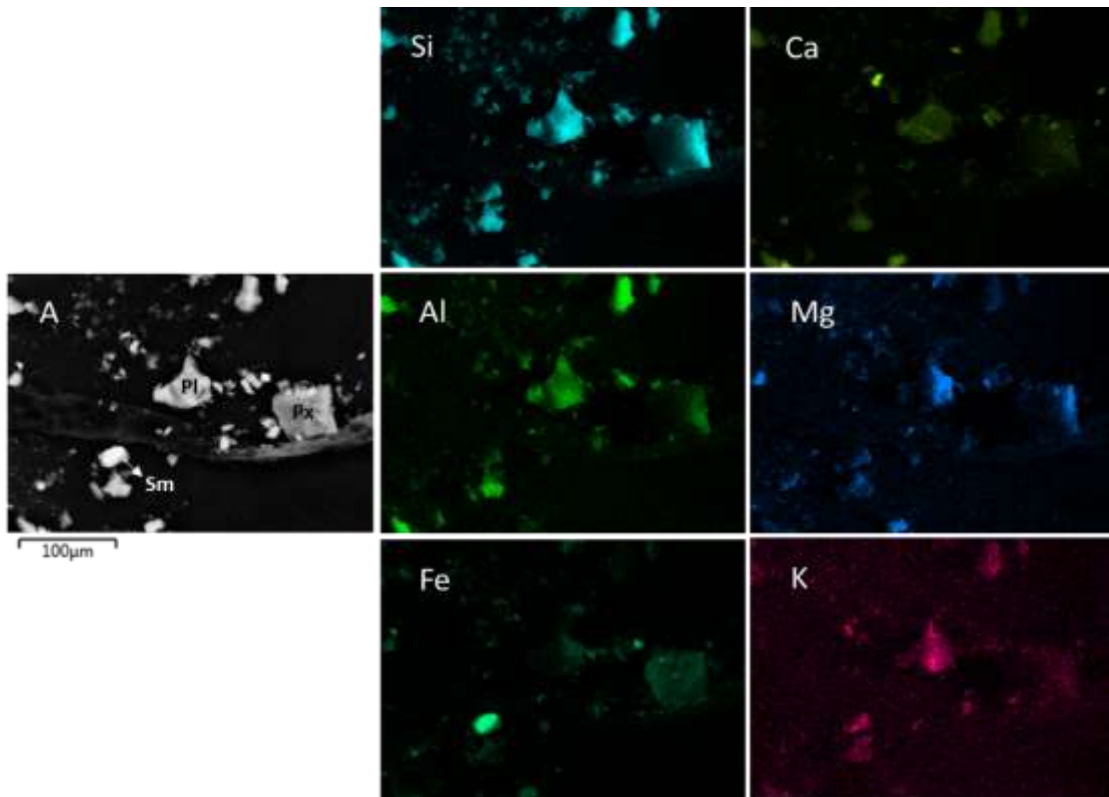


**Figure 3.** Energy-dispersive X-ray spectroscopy (EDS) images of basalt mineral compounds around maize root. A: secondary electrons image evidencing andesine (Pl), diopside (Px) and smectite (Sm) minerals; Si: silicon map; Al: aluminium map; Fe: iron map; Ca: calcium map; Mg: magnesium map; and K: potassium map.

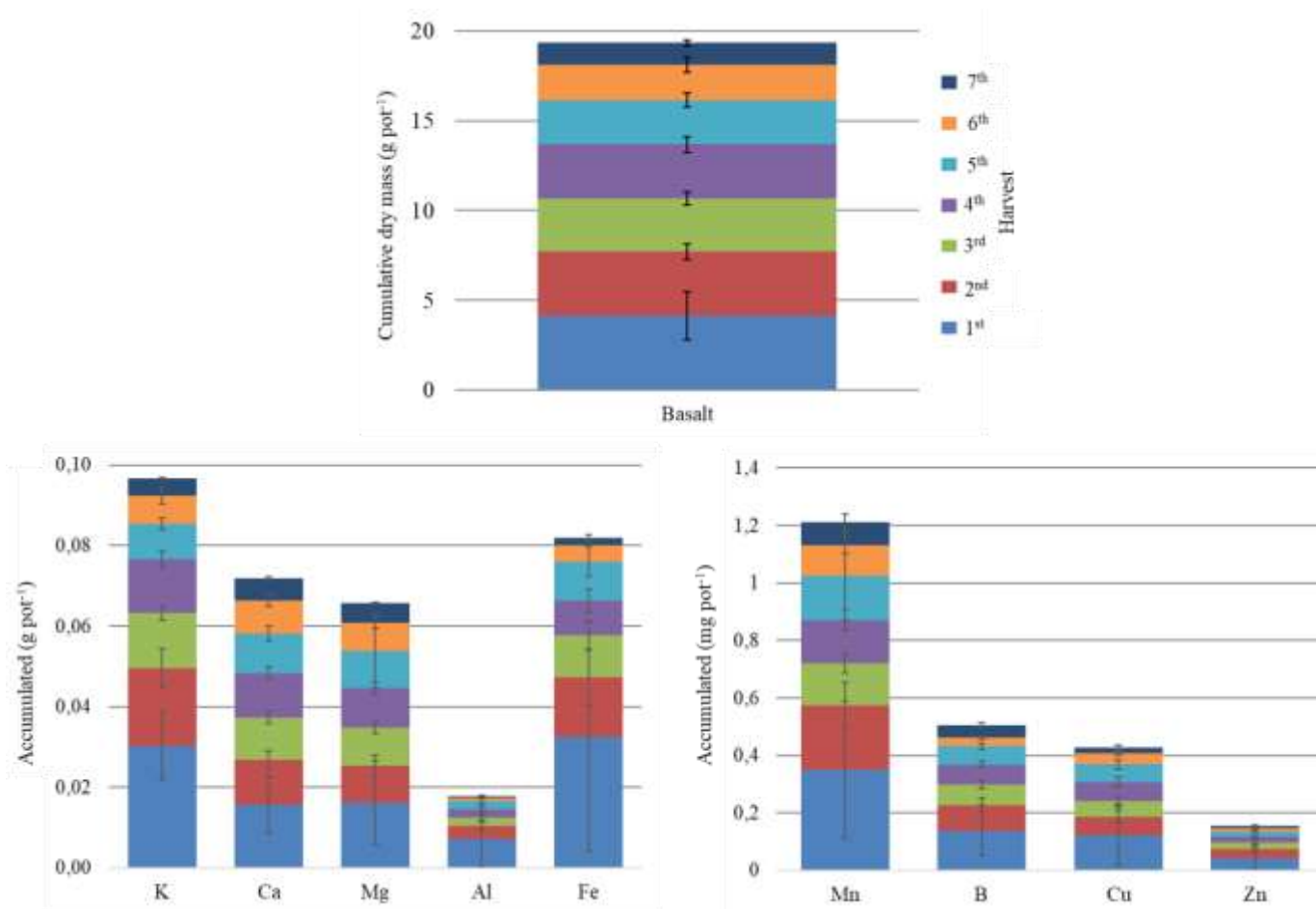


**Figure 4.** Cumulative dry mass and elements uptake<sup>1</sup> by maize cultivated in basalt power after seven cycles. <sup>1</sup>The number of samples per cycle used to calculate the mean ( $n$ ), from the 1<sup>st</sup> to the 7<sup>th</sup> cycle, was:  $n = 24 - i$ ; where  $i = \text{cycle number} * -3$ . Error bars for each cycle were the standard deviation of  $n$ .

(Malavolta et al., 1997). K offtake were in range between  $0.03 \text{ g pot}^{-1}$  from the first cycle to  $0.004 \text{ g pot}^{-1}$  to the last cycle (Figure 4, Equation 2).

$$K_{\text{offtake}} (\text{g per pot}) = 0.03^{**} - 0.0049^{**}(\text{cycle}), R^2 = 0.81 \quad (2)$$

Contents of Ca, Mg, Al and Fe in the maize tissue along the seven growth cycles indicated that nutrients were released from basalt minerals, and that basalt minerals were dissolved, partly due to a preferential dissolution of diopside.

The weathering of diopside and andesine in maize rhizosphere provided calcium and magnesium for plants. The nutrient concentration in dry mass ranged from  $2.3$  to  $5.3 \text{ g Ca kg}^{-1}$  and from  $1.3$  to  $6.6 \text{ g Mg kg}^{-1}$ . Calcium and magnesium requirement for maize growth was reached as concentration in maize leaves for optimum growth varies from  $2.5$  to  $4.0 \text{ g Ca kg}^{-1}$  (Malavolta et al., 1997), and from  $2.5$  to  $4.0 \text{ g Mg kg}^{-1}$  (Hawkesford et al., 2012). Calcium offtake was from  $0.015$  to  $0.005 \text{ g pot}^{-1}$  and Mg

was from  $0.016$  to  $0.004 \text{ g pot}^{-1}$ , from the first to the last cycle, respectively (Figure 4, Equations 3 and 4).

$$Ca_{\text{offtake}} (\text{g per pot}) = 0.015^{**} - 0.0042^{**}\ln(\text{cycle}), R^2 = 0.85 \quad (3)$$

$$Mg_{\text{offtake}} (\text{g per pot}) = 0.014^{**} - 0.0046^{**}\ln(\text{cycle}), R^2 = 0.80 \quad (4)$$

The decay in maize growth and in the offtake of elements is probably due to the weathering of surfaces and dissolution of very small mineral particles in the initial cycles, where nutrients were easily extractable, while in the subsequent cycles a higher effort seems to be made to extract and acquire nutrients from basalt minerals. The rhizosphere has an intrinsic role in basalt dissolution and release of elements. Akter and Akagi (2005) evaluated the active role of rhizosphere in basalt and showed that maize increased the Ca and Mg extraction by a factor of 3 - 4 and 15 - 75, respectively, when compared with the control pots with no plants. According to Hinsinger et al. (2001), the amounts of Ca, Mg and Na released from

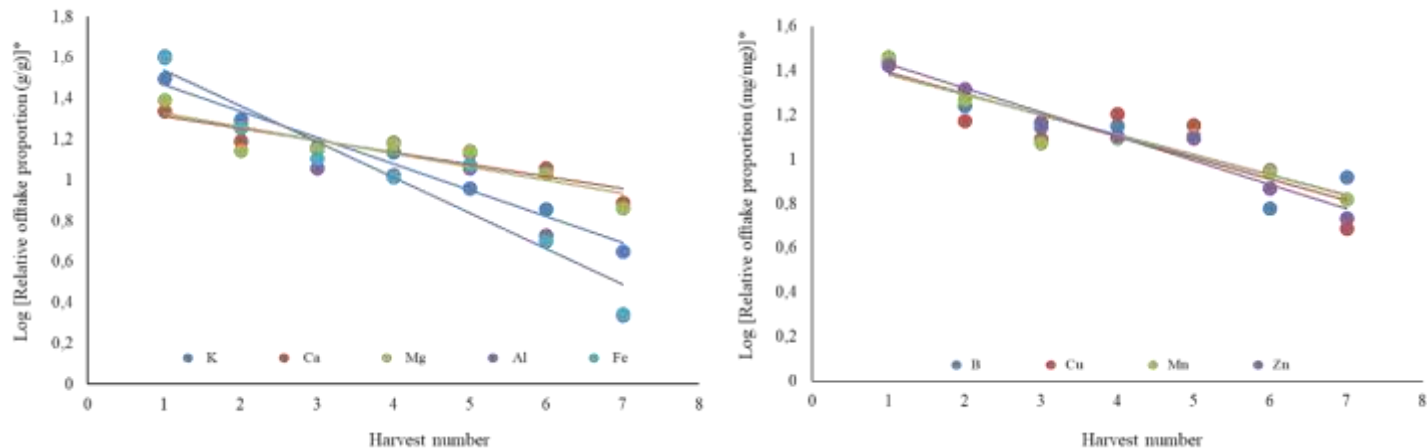


**Figure 5.** Elements offtake ratio from basalt by maize. \*Relative offtake proportion =  $\text{Log} \left[ \frac{\text{offtake} \cdot 100}{\sum_{c=1}^7 \left( \frac{\text{offtake}}{c} \right)} \right]$ ; c = harvest number.

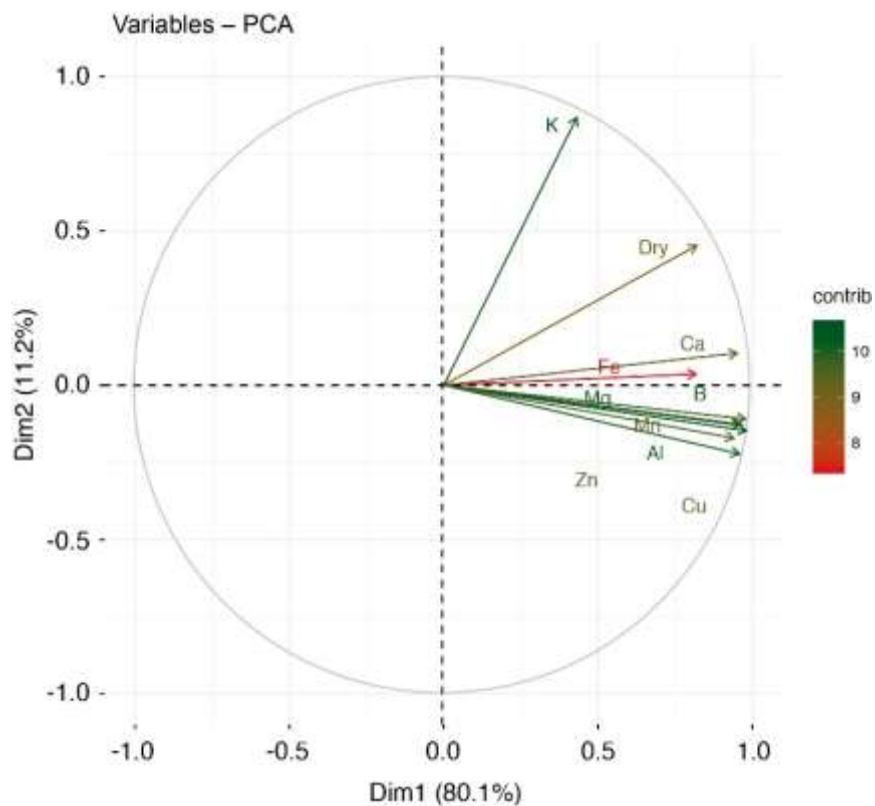


**Figure 6.** Principal component analysis of K, Ca, Mg, Fe, Al, Mn, B, Cu, and Zn maize offtake from basalt and cumulative. Dry = maize dry matter; Dim = dimension; Contrib = contribution.

basalt under leaching conditions in the laboratory increased by a factor ranging from 1 to 5 in the presence of crop plants.

The Al concentration in dry mass ranged from 0.2 to

3.5 g Al kg<sup>-1</sup>. Aluminum offtake along the cycles, although in a different scale, presented the same rate of Fe offtake (Figures 4 and 5). The Fe concentration ranged from 0.8 to 21.5 mg Fe kg<sup>-1</sup> and the concentration in maize leaves

for optimum growth varies from 50 – 250 mg Fe kg<sup>-1</sup> (Malavolta et al., 1997). In the course of the experiment, the offtake of these elements decayed (Equations 5 and 6). It suggests that ilmenite and diopside dissolution starts from iron oxidation during weathering, mainly from small particles and surfaces of lower crystallinity. As dissolution of easily weatherable minerals proceeds, along the cycles, Al, and Fe offtake decreases. Silva (2016) compared the dissolution of basalt at different grain sizes, despite not verifying the formation of new solid phases, confirmed the idea that the finer fractions are responsible for faster dissolution, while the coarser fractions dissolved slowly.

$$\text{Al}_{\text{offtake}} \text{ (g per pot)} = 0.01^{**} e^{(-0.47^{**} \text{cycle})}, R^2 = 0.91 \quad (5)$$

$$\text{Fe}_{\text{offtake}} \text{ (g per pot)} = 0.047^{**} e^{(-0.45^{**} \text{cycle})}, R^2 = 0.91 \quad (6)$$

The dissolution of small inclusions of ilmenite and diopside in basalt releases Fe. Strains of Fe-oxidizing bacteria are able to grow using the Fe(II) derived from ilmenite of basaltic rocks (Navarrete et al., 2013). This effect may be strongly influenced by the presence of organic acids from plants rhizosphere (Dontsova et al., 2014).

The water solubility of minerals containing Fe in soil is usually very low; however, plant and microbes, in the presence of organic substances, may work together for the oxidation and extraction of Fe(II) complexes, increasing Fe availability for plant growth (Colombo et al., 2014). In particular, gramineous species may have evolved, developing a very efficient mechanism to mobilize Fe (Broadley et al., 2012). According to Hinsinger et al. (2001), the amount of Fe released from basalt under leaching conditions using maize plants reached a maximum increase of about 100-500 times the release without plants (control). Non-absorbed iron ions in solution are then precipitated as low crystallinity iron oxides (especially ferrihydrite and amorphous ferric hydroxide) (Silva et al., 2017).

Images of basalt samples obtained by SEM after the last crop cycle show the interaction between roots and mineral particles, including low crystalline structures (Figure 7). These structures are known as short-range ordered (SRO) minerals like ferrihydrite. Long-term field studies conducted by Yu et al. (2017) demonstrated that the presence of roots significantly increased Al and Fe availability from soils.

This result challenges the conceptual view that the weathering and the formation of SRO minerals are very slow processes and cannot be detected in the short-term (Colombo et al., 2014; Yu et al., 2017). It suggests that the dissolution of minerals can be accelerated by plant roots.

Offtake of manganese, boron, copper, and zinc showed a similar trend when normalized (Figures 4 and 5), although were taken up in different proportions by plants.

The micronutrients Mn, B and Zn are present indistinctively in all primary minerals that compose this basalt, especially diopside (Morales et al., 2018), while Cu is accumulated in smectite structure, formed by hydrothermal process (Baggio et al., 2016).

Manganese undertakes a similar oxidation process than Fe in mineral structures during weathering, releasing other elements. Manganese concentration values in maize tissue varied from 35 to 159 mg Mn kg<sup>-1</sup>, while the sufficiency range for maize is from 50 to 150 mg Mn kg<sup>-1</sup> (Malavolta et al., 1997). The Mn offtake varied from 0.35 to 0.07 mg pot<sup>-1</sup>, from the first to the last cycle, respectively (Figure 4), and decayed according to the Equation 7.

$$\text{Mn}_{\text{offtake}} \text{ (mg per pot)} = 0.32^{**} - 0.12^{**} \ln(\text{cycle}), R^2 = 0.92 \quad (7)$$

Boron concentration values in maize ranged between 13.5 to 76.7 mg B kg<sup>-1</sup>, while the adequate level for maize is from 15 to 20 mg B kg<sup>-1</sup> (Malavolta et al., 1997). For maize, the critical toxicity concentrations in leaves are in the range of 100 mg kg<sup>-1</sup> (Broadley et al., 2012); therefore, in the case where the basalt is applied to soils, it does not represent any risk of soil contamination with B, but a source of nutrient. In the course of experiment, B offtake ranged from 0.13 to 0.04 mg pot<sup>-1</sup> from first and the last cycle (Figure 4) and decayed according to the Equation 8.

$$\text{B}_{\text{offtake}} \text{ (mg per pot)} = 0.13^{**} - 0.049^{**} \ln(\text{cycle}), R^2 = 0.92 \quad (8)$$

Copper offtake was higher in the first cycle, media of 120 mg pot<sup>-1</sup>, and decreased to 20 mg pot<sup>-1</sup> in the last (Figure 4, Equation 9) but shows an adequate Cu concentration in all cycles (mean 23.5 mg Cu kg<sup>-1</sup>). The critical level concentration of Cu in maize is generally between 6 to 20 mg Cu kg<sup>-1</sup> (Malavolta et al., 1997) and no visible toxicity symptoms of Cu were noticed.

$$\text{Cu}_{\text{offtake}} \text{ (mg per pot)} = 0.11^{**} - 0.041^{**} \ln(\text{cycle}), R^2 = 0.79 \quad (9)$$

Zinc concentration in maize dry matter were below the critical level [15 – 50 mg Zn kg<sup>-1</sup> (Broadley et al., 2012)]. Zinc offtake was the lowest among micronutrients, reflecting the content of the element in the basalt. Zinc offtake decayed from 0.04 to 0.08 mg pot<sup>-1</sup>, from the first to the last cycle (Figure 4), following the Equation 10.

$$\text{Zn}_{\text{offtake}} \text{ (mg per pot)} = 0.04^{**} - 0.016^{**} \ln(\text{cycle}), R^2 = 0.97 \quad (10)$$

## Conclusion

The basalt mineralogical composition did not change along the experiment, because the dissolution of basalt in maize rhizosphere was congruent. The smectite present in the basalt contributed to the high cationic exchange

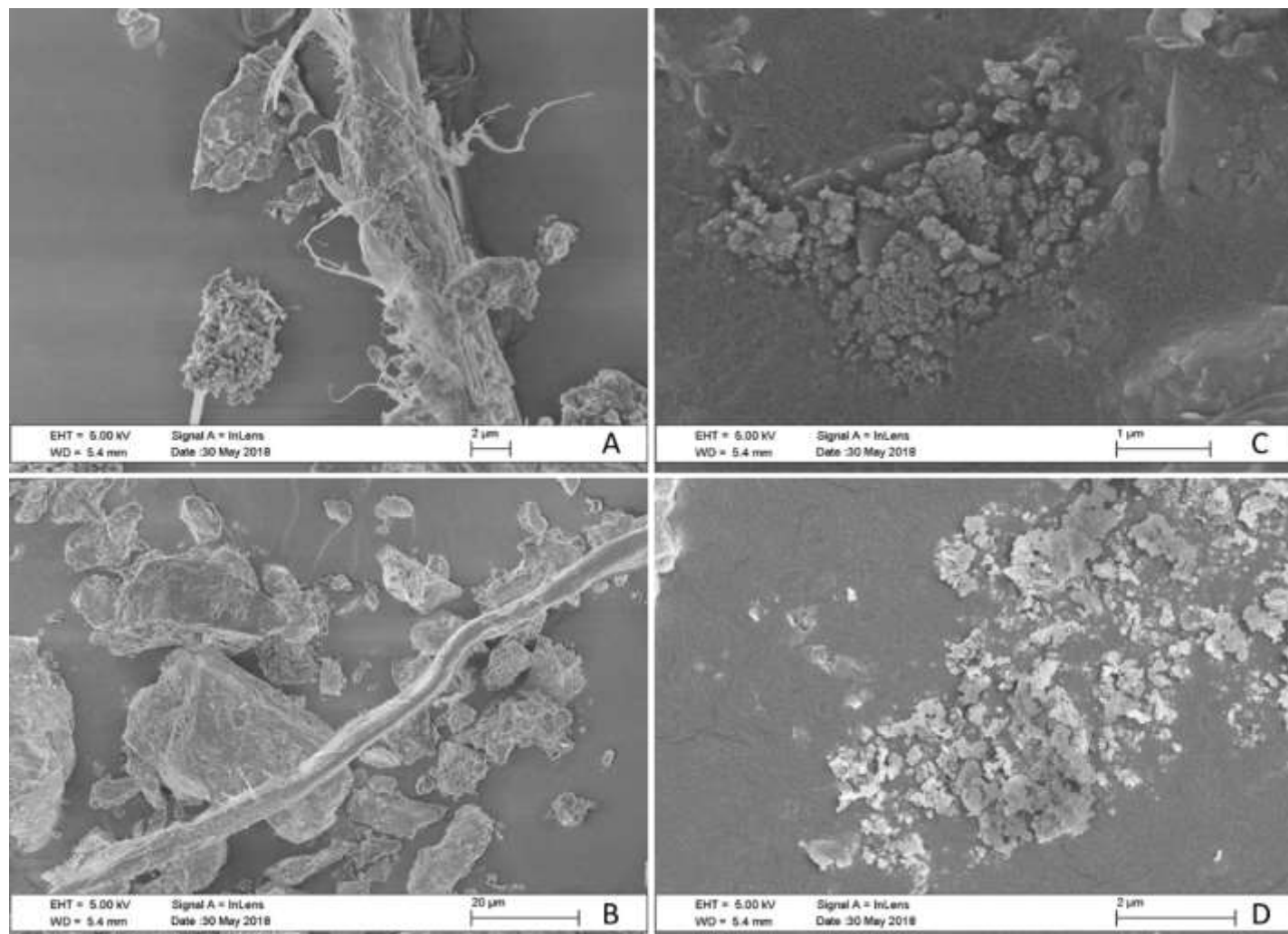


**Figure 7.** Scanning electron microscopy images of basalt samples after seven maize growth cycles. A and B: interaction of roots with basalt minerals; C and D: deposits of low crystallinity minerals.

capacity, indicating a possible ability to change cations into soil environment. Therefore, applications of basalt in Cerrado Oxisols can improve soil quality by adding permanent charge and by increasing its overall CEC. Basalt was able to provide nutrients to maize plants in a short period. Additionally, the offtake rate of elements from basalt was described by equations, which may be used for estimating nutrients release from basalt after being applied in agricultural soils.

#### CONFLICT OF INTERESTS

The authors have not declared any conflict of interests.

#### FUNDING

This study was financed in part by the Coordenação de

Aperfeiçoamento de Pessoal de Nível Superior - Brasil (CAPES) - Finance Code 001, and Fundação de Apoio à Pesquisa do Distrito Federal (FAPDF) grant nº 0193-001.478/2016.

#### ACKNOWLEDGEMENTS

The authors acknowledge the Universidade de Brasília - UnB, Embrapa Cerrados, Embrapa Agroenergia and Universidade Federal do Pará - UFPA.

#### REFERENCES

- Akter M, Akagi T (2005). Effect of fine root contact on plant-induced weathering of basalt. *Soil Science and Plant Nutrition* 51(6):861-871.
- Anda M, Shamshuddin J, Fauziah CI (2015). Improving chemical properties of a highly weathered soil using finely ground basalt rocks. *Catena* 124(1):147-161.

- Baggio SB, Hartmann LA, Bello RMS (2016). Paralavas in the Cretaceous Paraná volcanic province, Brazil – A genetic interpretation of the volcanic rocks containing phenocrysts and glass. *Anais da Academia Brasileira de Ciências* 88(4):2167-2193.
- Basak BB (2018). Waste Mica as Alternative Source of Plant-Available Potassium: Evaluation of Agronomic Potential Through Chemical and Biological Methods. *Natural Resources Research* 28(3):953-965.
- Berner RA, Schott J (1982). Mechanism of pyroxene and amphibole weathering II. Observations of soil grains. *American Journal of Science* 282(8):1214-1231.
- Bray AW, Oelkers EH, Bonneville S, Wolff-Boenisch D, Potts NJ, Fones G, Benning LG (2015). The effect of pH, grain size, and organic ligands on biotite weathering rates. *Geochimica et Cosmochimica Acta* 164(1):127-145.
- Broadley M, Brown P, Cakmak I, Rengel Z, Zhao F (2012). Function of Nutrients: Micronutrients. In: Marschner P (Ed.), *Marschner's Mineral Nutrition of Higher Plants*. London: Academic Press, pp. 191-248.
- BS EN ISO 11260 (2011). Soil Quality: determination of Effective Cation Exchange Capacity and Base Saturation Level using Barium Chloride Solution. B. Standards.
- Burghilea C, Zaharescu DG, Dontsova K, Maier R, Huxman T, Chorover J (2015). Mineral nutrient mobilization by plants from rock: influence of rock type and arbuscular mycorrhiza. *Biogeochemistry* 124(1):187-203.
- Campos-MM, Campos-CR (2017). Applications of quartering method in soils and foods. *Journal of Engineering Research and Application* 7(1):35-39.
- Chaturika JAS, Indraratne SP, Dandeniya WS, Kumaragamage D (2015). Beneficial management practices on growth and yield parameters of maize (*Zea mays*) and soil fertility improvement. *Tropical Agricultural Research* 27(1):59-74.
- Ciceri D, Allanore A (2019). Local fertilizers to achieve food self-sufficiency in Africa. *Science of the Total Environment* 64(1):8669-680.
- Colombo C, Palumbo G, He JZ, Pinton R, Cesco S (2014). Review on iron availability in soil: interaction of Fe minerals, plants, and microbes. *Journal of Soils and Sediments* 14(3):538-548.
- Dontsova K, Zaharescu, D, Henderson W, Verghese S, Perdrial N, Hunt E, Chorover J (2014). Impact of organic carbon on weathering and chemical denudation of granular basalt. *Geochimica et Cosmochimica Acta* 139(1):508-526.
- Eggleton RA, Foudoulis C, Varkevissier D (1987). Weathering of basalt: changes in rock chemistry and mineralogy. *Clays and Clay Minerals* 35(3):161-169.
- Embrapa (2017). Manual de métodos de análise de solo. Rio de Janeiro: Centro Nacional de Pesquisa de Solos 1(2):212.
- Essington ME (2003). Soil and water chemistry: an integrative approach. Boca Raton: CRC PRESS 181(1):656.
- Hawkesford M, Horst W, Kichey T, Lambers H, Schjoerring J, Møller IS, White P (2012). Functions of Macronutrients. In: Marschner P (Ed.), *Marschner's Mineral Nutrition of Higher Plants*. London: Academic Press, pp. 135-189.
- Hinsinger P, Barros ONF, Benedetti MF, Noack Y, Callot G (2001). Plant-induced weathering of a basaltic rock: Experimental evidence. *Geochimica et Cosmochimica Acta* 65(1):137-152.
- Lefebvre D, Goglio P, Williams A, Manning DAC, Azevedo AC, Bergmann M, Meersmans J, Smith P (2019). Assessing the potential of soil carbonation and enhanced weathering through Life Cycle Assessment: A case study for Sao Paulo State, Brazil. *Journal of Cleaner Production* 233(1):468-481.
- Malavolta E, Vitti GC, Oliveria SA (1997). Avaliação do estado nutricional das plantas: princípios e aplicações. POTAFOS P. 319.
- Manning DAC, Baptista J, Limon MS, Brandt K (2017). Testing the ability of plants to access potassium from framework silicate minerals. *Science of the Total Environment* 574(1):476-481.
- Marchi G, Vilar CC, O'Connor G, Silva MLN (2015). Surface Complexation Modeling in variable charge soils: charge characterization by potentiometric titration. *Revista Brasileira de Ciência do Solo* 39(5):1387-1394.
- Moraes LC, Seer HJ, Marques LSM (2018). Geology, geochemistry and petrology of basalts from Paraná Continental Magmatic Province in the Araguari, Uberlândia, Uberaba and Sacramento regions, Minas Gerais state, Brazil. *Brazilian Journal of Geology* 48(2):221-241.
- Navarrete JU, Cappelle IJ, Schnittker K, Borrok DM (2013). Bioleaching of ilmenite and basalt in the presence of iron-oxidizing and iron-scavenging bacteria. *International Journal of Astrobiology* 12(2):123-134.
- Nunes JMG, Kautzmann RM, Oliveira C (2014). Evaluation of the natural fertilizing potential of basalt dust wastes from the mining district of Nova Prata (Brazil). *Journal of Cleaner Production* 84(1):649-656.
- Paktunk AD (1998). MODAN: an interactive computer program for estimating mineral quantities based on bulk composition. *Computers and Geosciences* 24(5):425-431.
- Raheb A, Heidari A (2011). Clay mineralogy and its relationship with potassium forms in some paddy and non-paddy soils of northern Iran. *Australian Journal of Agricultural Engineering* 2(6):169-175.
- Ramos CG, Querol X, Oliveira MLS, Pires K, Kautzmann RM, Oliveira LFS (2015). A preliminary evaluation of volcanic rock powder for application in agriculture as soil a remineralizer. *Science of the Total Environment* 512-513:371-380.
- Samal D, Kovar JL, Steingrobe B, Sadana US, Bhadoria PS, Claassen N (2010). Potassium uptake efficiency and dynamics in the rhizosphere of maize (*Zea mays* L.), wheat (*Triticum aestivum* L.), and sugar beet (*Beta vulgaris* L.) evaluated with a mechanistic model. *Plant and Soil* 332(2):105-121.
- Silva RCS (2016). Intemperismo de minerais de um remineralizador. PhD. Escola Superior de Agricultura Luiz de Queiroz, Piracicaba: 183.
- Silva RCS, Cury ME, Ieda JJC, Sermarini RA, Azevedo AC (2017). Chemical attributes of a remineralized Oxisol. *Ciência Rural* 47(11):1-10.
- Wang JG, Zhang FS, Cao YP, Zhang XL (2000). Effect of plant types on release of mineral potassium from gneiss. *Nutrient Cycling in Agroecosystems* 56(1):37-44.
- Wilson MJ (2004). Weathering of the primary rockforming minerals: Processes, products and rates. *Clay Minerals* 39(3):233-266.
- Yu G, Xiao J, Hu S, Polizzotto ML, Zhao F-J, Mcgrath SP, Li H, Ran W, Shen Q (2017). Mineral availability as a key regulator of soil carbon storage. *Environmental Science and Technology* 51(9):4960-4969.
- Zorb C, Senbayram M, Peiter E (2014). Potassium in agriculture-status and perspectives. *Journal of Plant Physiology* 171(9):656-669.